Fabrication and Characterization of Clay/epoxy nanocomposite

Farhana Pervin, Yuanxin Zhou, Mohammad A. Biswas, Vijaya K. Rangari, Shaik Jeelani
Tuskegee University's Center for Advanced Materials (T-CAM)
Tuskegee, AL 36088, USA

Abstract

In the present investigation we have developed a novel technique to fabricate nanocomposite materials containing SC-15 epoxy resin and K-10 montmorillonite clay. A high intensity ultrasonic liquid processor was used to obtain a homogeneous molecular mixture of epoxy resin and nano clay. The clays were infused into the part A of SC-15 (Diglycidylether of Bisphenol A) through sonic cavitations and then mixed with part B of SC-15 (cycloaliphatic amine hardener) using a high speed mechanical agitator. The trapped air and reaction volatiles were removed from the mixture using high vacuum. DMA, TGA and 3-point bending tests were performed on unfilled, 1wt. %, 2wt. %, 3% and 4wt. % clay filled SC-15 epoxy to identify the loading effect on thermal and mechanical properties of the composites. The flexural results indicate that 2.0 wt% loading of clay in epoxy resin showed the highest improvement in flexural strength as compared to the neat systems. DMA studies also revealed that 2.0 wt% doped system exhibit the highest storage modulus and Tg as compared to neat and other loading percentages. However, TGA results show that thermal stability of composite is insensitive to the clay content.

INTRODUCTION

Traditional fiber-reinforced composites have improved over the years with respect to their material properties and have gained considerable acceptance in the aerospace industry. Generally, the in-plane properties of the fiber/polymer composite are defined by the fiber properties, while the properties along the thickness dimension are defined by the characteristics of the matrix resin. Epoxy resin is the most commonly used polymer matrix with reinforcing fibers for advanced composites applications. The resins of this class have good stiffness, specific strength, dimensional stability, chemical resistance, and show considerable adhesion to the embedded fiber [1]. Using an additional phase (e.g. inorganic fillers) to strengthen the properties of epoxy resins has become a common practice [2]. The use of these fillers has been proven to improve the mechanical properties of epoxy resins. Based on the fact that micro scale fillers have successfully been synthesized with epoxy resin [3-6], nano-scaled clay are now being considered as filler material to produce high performance composite structures with further enhanced properties.

Nano-phased matrix based on organic polymers and inorganic clay minerals consisting of silicate layers such as montmorillonite (MMT) have attracted great interest because they frequently exhibit unexpected properties including reduced gas permeability, improved solvent resistance, superior mechanical and enhanced flame-retardant properties [7-12]. Different polymer/clay nanocomposites have been successfully synthesized by incorporating clay in various polymer matrixes such as,

polyamides[13], polyamides [14], epoxy [15], polyurethane [16], poly(ethylene terephthalate) [17] and polypropylene [18].

The primary interest of this paper was to characterize the effect of K-10 montmorillonite clay on the thermal and mechanical properties of SC-15 epoxy. An ultrasonicator was used to process clay-epoxy nanocomposite. Flexural tests were performed to evaluate mechanical performance. Thermogravimetric Analysis (TGA) and Dynamic Mechanical Analysis (DMA) were performed to evaluate the thermal performances. Microscopic approaches were used to investigate the fracture behavior and mechanism of material. Based on experimental results, a nonlinear constitutive equation was developed to describe the stress-strain relationship of material.

EXPERIMENTAL

Materials and Manufacturing of Nanocomposites:

The resin used in this study is a commercially available SC-15 epoxy obtained from *Applied Poleramic, Inc.* It is a low viscosity two phased toughened epoxy resin system consisting of part-A (resin mixture of Diglycidylether of Bisphenol-A, Aliphatic Diglycidylether epoxy toughner) and part-B (hardener mixture of, cycloaliphatic amine and polyoxylalkylamine). The inorganic clay, used in this study, was K-10 grade montorillonite obtained from Sigma-Aldrich Co. (USA) with a surface area 220-270m^2/g. The weight fraction of clay are range from 0 wt. % to 4 wt. % to identify an optimal loading giving the best thermal and mechanical properties.

Firstly, clay was dried in oven at a temperature of 80 ^oC for 24 hours. Then pre-calculated amount of clay and part-A resin were carefully weighted, and mixed together in a suitable beaker. The mixing was carried out through a high intensity ultrasonic irradiation (Ti-horn, 20 kHz *Sonics Vibra Cell, Sonics Mandmaterials, Inc, USA)* for one and half hour with pulse mode (50sec. on/ 25sec. off) since part-A is insensitive to ultrasound irradiation. To avoid a temperature rise during the sonication process, external cooling was employed by submerging the beaker containing the mixture in an ice-bath. Once the irradiation was completed, part-B was added to the modified part-A then mixed using a high speed mechanical stirrer for about 10 minutes. The mix-ratio of part A and part B of SC-15 is 10:3. The rigorous mixing of part-A and part-B produced highly reactive volatile vapor bubbles at initial stages of the reaction, which could detrimentally affect the properties of the final product by creating voids. A high vacuum was accordingly applied using *Brand Tech Vacuum* system for about 30 minutes. After the bubbles were completely removed, the mixture was transferred into a plastic and Teflon coated metal rectangular molds and kept for 24 hours at room temperature. The cured material was then de-molded and trimmed. Finally, test samples were machined for thermal and mechanical characterization. All as-prepared panels were post-cured at 100°C for five hours, in a Lindberg/Blue Mechanical Convection Oven. The block diagram for manufacturing of clay/epoxy nanocomposite is shown in Figure 1.

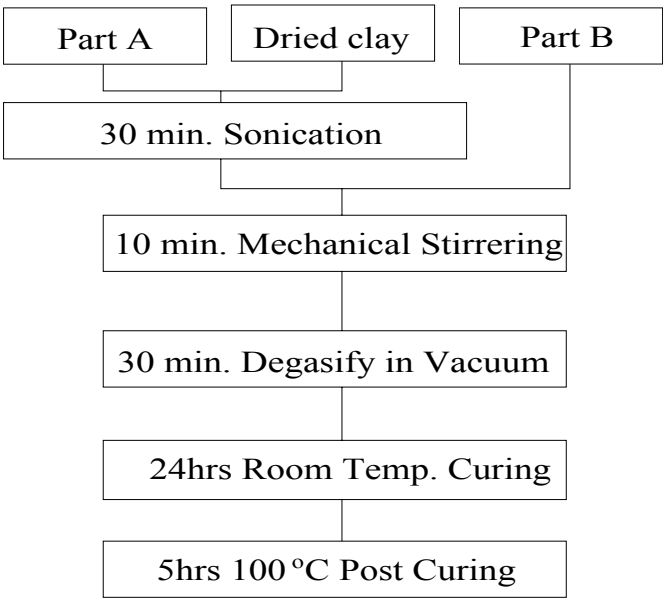

Figure 1 Fabrication of caly/epoxy nanocomposite

Test Procedure

Dynamic Mechanic analysis (DMA) was performed on a TA Instruments 2980 operating in the three-point bending mode at an oscillation frequency of 1Hz. Data were colleted from room temperature to 160°C at a scanning rate of 10°C/min. The sample specimens were cut by a diamond saw in the form of rectangular bars of a nominal $4mm \times 30mm \times 12mm$. Thermo gravimetric Analysis (TGA) was conducted with a TA Instruments TGA2950 at a heat rate of 10°C/min from ambient to 600°C. The TGA samples were cut into small pieces using ISOMET Cutter and were machined using the mechanical grinder to maintain the sample weight of about 5-20mg range. These samples were sealed in aluminum crucibles and placed inside the apparatus. The real time characteristic curves were generated by *Universal Analysis 2000-TA Instruments Inc.,* data acquisition system.

Flexural tests under three point bend configuration were performed according to ASTM D790-86. The tests were conducted in a 10 KN servo hydraulic testing machine (MTS) equipped with Test Ware data acquisition system. The machine was run under displacement control mode at a cross head speed of 2.0 mm/min, and all the tests were performed at room temperature. Test samples were cut from the panels using a Felker saw fitted with a diamond coated steel blade. Five replicate specimens from four different materials were prepared for static flexure tests.

RESULTS AND DISCUSSIONS

Thermal properties

Figure 2 illustrates the DMA plots of storage modulus versus temperature as a function of clay loading. It can be seen that the storage modulus steadily increases with an increasing clay content up to 2%. Above 2%, the storage modulus decreased with increasing clay content. The addition of 2 wt. % of clay yielded a 58% increase of the storage modulus at 30°C. The loss factor, $\tan\delta$, curve of the neat epoxy and its

clay/epoxy nanocomposites measured by DMA are shown in Figure 3. The maximum Tg, determined from the peak position of tan δ, was observed at 3 wt. % clay system. 3^{o}C enhancement in Tg has been found. In Figure 3, the peak height of loss factor decreased with increasing clay content, but width of tan δ is insensitive to the clay content. The peak factor, Γ, is defined as the full width at half maximum of the tan δ peak devided by its height, can be qualitatively used to assess the homogeneity of epoxy network[]. The neat epoxy was observed to have a low peak factor that indicates that the crosslink density and homogeneity of the epoxy network were high. For the nanocomposites, the peak factor increased with increasing clay weight percent, as shown in Figure 4, and exhibited a broadened tan δpeak on the high temperature side of the DMA profile. The higher peak factor for the nanocomposites is indicative of lower crosslink density and greater heterogeneity, which suggests intercalation of the epoxy network into the clay layers.

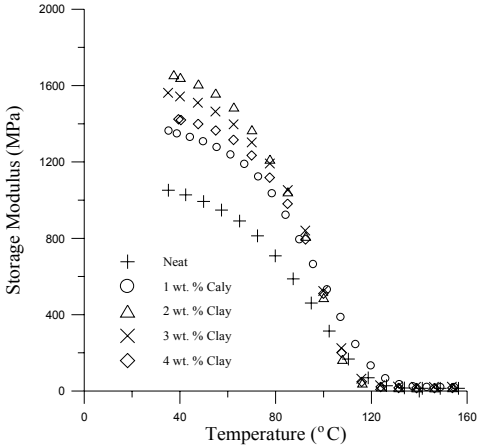

Fig. 2 Storage modulus versus temperature plots of clay-epoxy nanocomposite

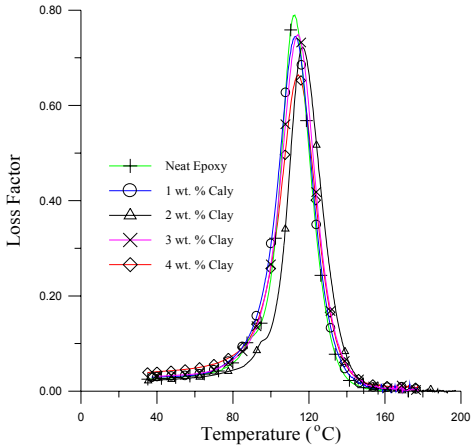

Fig. 3 Loss factor versus temperature plots of clay-epoxy nanocomposite

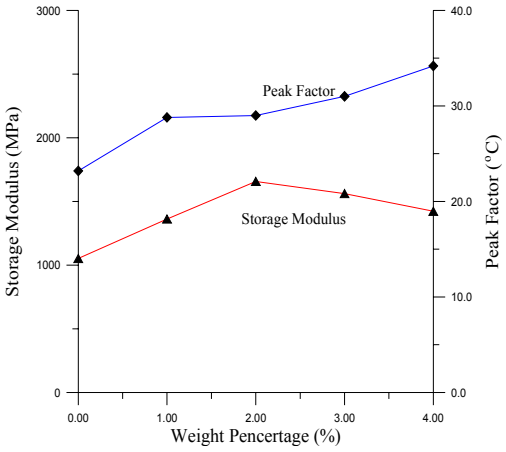

Fig. 4 Effect of clay content on storage modulus and peak factor of material

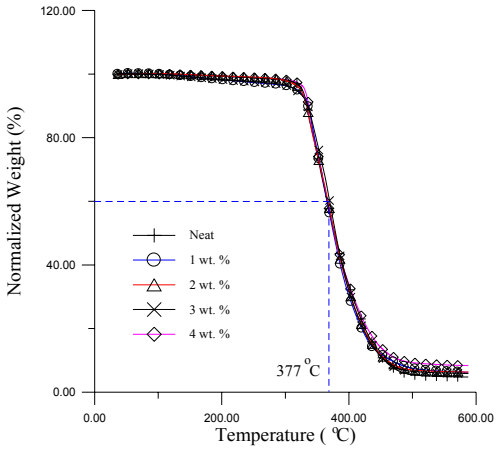

Fig. 5 TGA results of clay-epoxy nanocomposite

Thermo gravimetric analysis (TGA) measurements were also carried out to obtain information on the thermal stability of the various nanocomposite systems. Figures 5 shows the TGA of all categories of nanocomposites considered for this investigation. We define the 50% weight loss as a marker for structural decomposition of the samples. In this figure, the decomposition temperatures are almost the same, indicating the clay contents have no effect on the decomposition temperature of epoxy.

Table 1. Effects of clay content on the mechanical and thermal properties of epoxy and its nano composite

Material	Modulus (GPa)	Improvement in modulus	Strength (MPa)	Improvement in strength
Neat Epoxy	2.25 ± 0.11	--------	85 ± 4.3	--------
1 wt. % clay	2.58 ± 0.12	14.7%	94 ± 5.9	10.6%
2 wt. % clay	2.96 ± 0.14	31.6%	108 ± 5.6	27.1%
3 wt. % clay	2.70 ± 0.14	20.0%	105 ± 4.6	23.5%
4 wt. % clay	2.43 ± 0.11	8.0%	104 ± 4.1	23.5%

Flexural Response

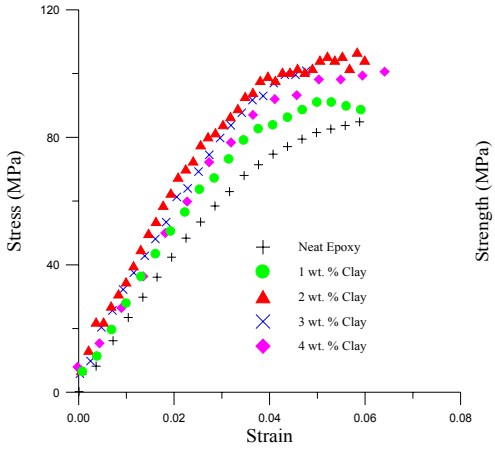

Fig. 6 Stress-strain curves of materials

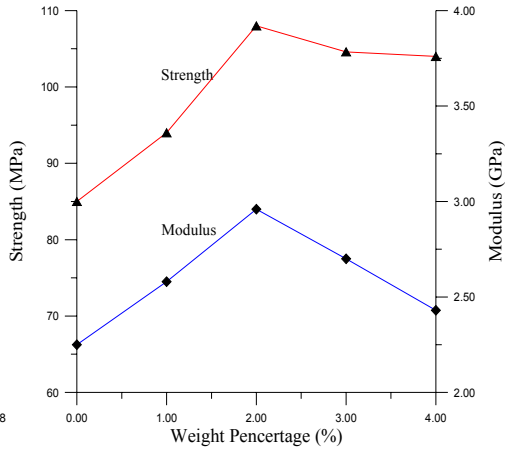

Fig. 7 Effect of clay content on properties

Flexural tests were performed to evaluate the bulk stiffness and strength of epoxy and its nano-composites. Typical stress strain behavior from the flexural tests is shown in Figure 6. All specimens failed immediately after the stress reached the maximum value; however, the stress-strain curves showed considerable non-linearity before reaching the maximum stress, but no obvious yield point was found in the curves. Five specimens were tested for each condition. The average properties obtained from these tests are listed in Table 1. Figure 7 shows the variation of modulus and strength with clay content.

Optimal loading of clay was found at 2wt. %, and an improvement of about 32% in modulus and 27% in strength were observed with an addition of 2 wt.% of caly.

Fracture Surface

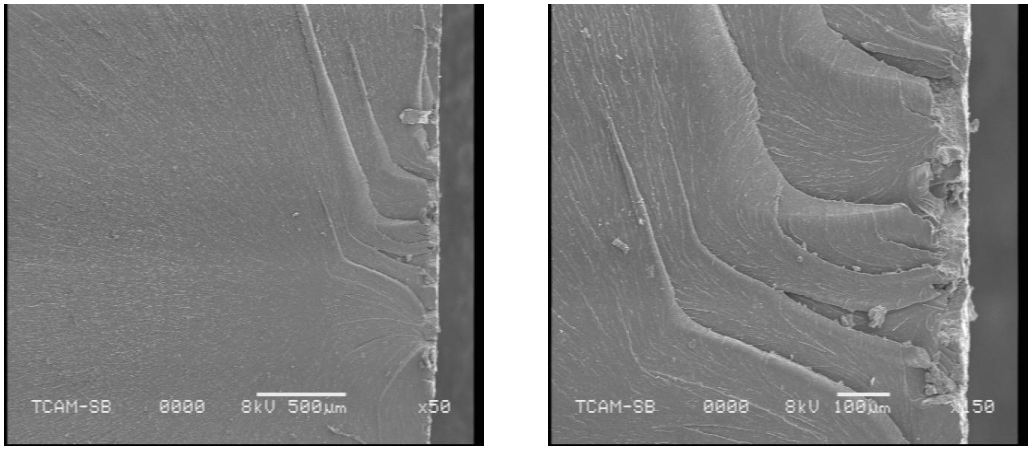

A B

Figure 8 Fracture surface of neat epoxy (A: initial crack occurred at the tensile edge of specimen; B: typical cleavage feature)

The fracture surfaces of neat epoxy and the nanocomposites were comparatively examined using SEM. It can be seen in Figure 8a that neat epoxy resin exhibits a relatively smooth fracture surface and initial crack occurred at the tension edge of specimen. Higher magnification SEM picture in Figure 8b indicates a typical fractography feature of brittle fracture behavior, thus accounting for the low fracture toughness of the unfilled epoxy.

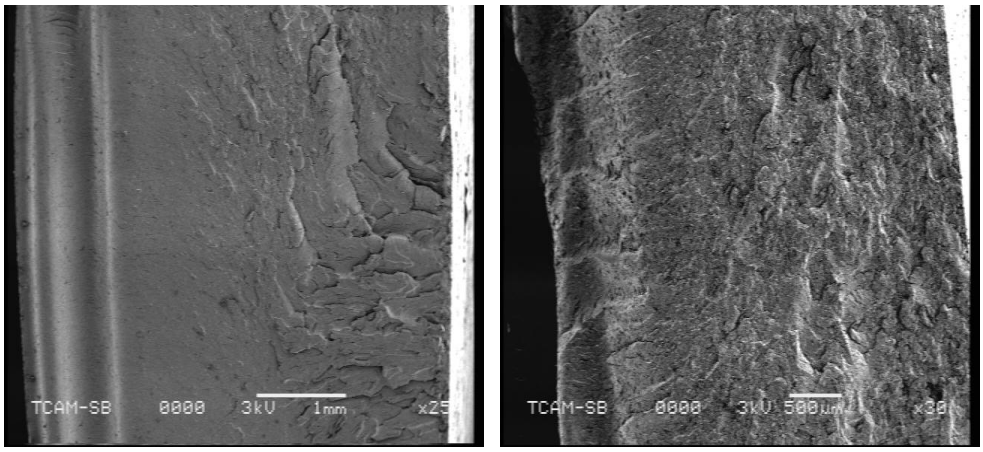

A B

Figure 8 Initial crack occurred at the tension edge of clay/epoxy nanocomposite (A: 2 wt. % clay; B: 4 wt. % clay)

Compared to the case of neat epoxy, the fracture surfaces of the nanocomposites show considerably different fractographic features. As a representative example, the failure surface of the nanocomposite containing 2 wt. % clay and 4 wt. % clay are shown in Figure 9a and 9b. Generally, a much rougher fracture surface is seen upon adding clay into the epoxy matrix.

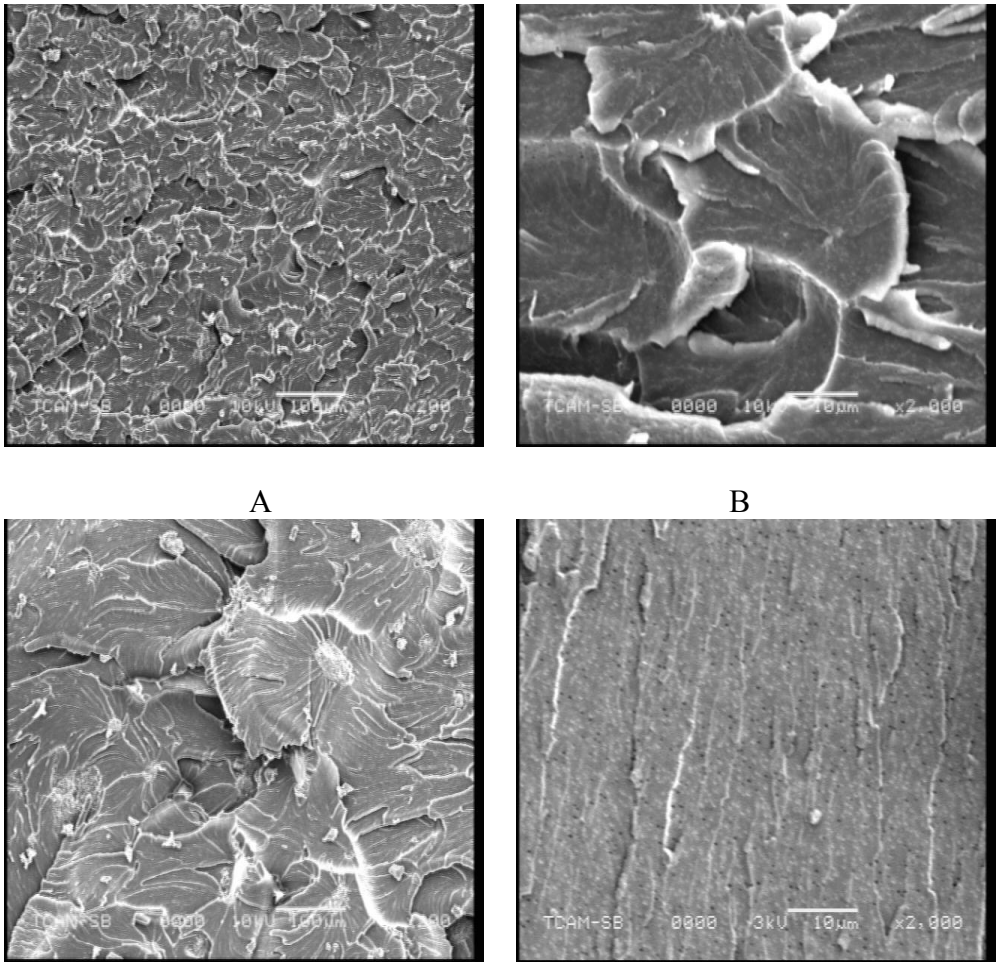

Figure 10 Dispersions of clay in the epoxy
(A: 2wt%; B: 2wt%, C: 4 wt.% and D: neat epoxy)

Figure 10a-c show the micrograph of clay-epoxy composite. The micrograph clearly indicates that , for 2 wt. % system, the clays are well dispersed in the resin. The clays are well separated and uniformly embedded in the epoxy resin. Higher magnification SEM picture in Figure 10b shows that no agglomerated particles was observed. But for 4 wt.% clay-epoxy composite, large size particles are found at the fracture surface. These large size particles are formed by the agglomeration of nano-clay. The crack initiation was caused by the stress concentration caused by the agglomerated particle. Figure 10d shows the fracture surface of neat epoxy. Many small dots scattered across the fracture surface of specimen. The SC-15 epoxy is similar to a second-phase

rubber-toughened epoxy. These dots were caused by toughening rubber particles at fracture surface.

CONCLUSION

K-10 montmorillonite clay has been infused in SC-15 epoxy by ultrasonic cavitation method. DMA results exhibited 58% improvement in storage modulus for 2 wt.% clay/epoxy system. TGA results show that the clay content has no effect on the decomposition temperature. The flexural results indicate that 2.0 wt% loading of clay in epoxy resin showed the highest improvement in flexural strength as compared to the neat systems. 31.6% improvement in modulus and 27% improvement in strength were observed with an addition of 2 wt. % of clay.

Acknowledgements

The authors would like to gratefully acknowledge the support of National Science Foundation through grant no.: HRD-0317741.

Reference

1. Y. Zheng, Y. Zheng, R. Ning, Materials Letters, **57,** (2003) pp 2940-2944.
2.R. J. Day, P. A. Lovell, A. A. Wazzan,. Composites Science and Technology, **61** (2001) pp 41-56.
3. Bagheri, R. A. Pearson, Polymer, **41** (2001) pp 269-276.
4 T. Kawaguchi, R. A. Pearson, Polymer, **44** (2003) pp 4239-4247.
5. Mahfuz, A. Adnan, V. K. Rangari, S. Jeelani, and B. Z. Jang, Composites: Part A: pplied science and manufacturing, **35** (2004) pp 519-527.
6. M.F. Evora, A. Shukla, Materials Science & Engineering, **A361**: (2003) pp 358-366.
7. K. Yano, A. Uzuki, A. Okada, T. Kurauchi and O. Kamigaito, *Journal Polym Sci Part A: Polym Chem* **31** (1993), p. 2493.
8. R.A. Via, H. Ishii and E.P. Giannelis, *Chem Mater* **5** (1993), p. 1694.
9. P.B. Messersmith and E.P. Giannelis, *J Polym Sci Part A: Polym Chem* **33** (1995), p. 1047.
10. R. Krishnamoorti, R.A. Vaia and E.P. Giannelis, *Chem Mater* **8** (1996), p. 1728.
11. M. Kawasumi, N. Hasegawa, M. Kato, A. Usuki and A. Okada, *Macromolecules* **30** (1997), p. 6333.
12. D. F. Wu, C. X. Zhou. X. Fan, D. L. Mao and Z. Bian, Polymer Degradation and Stability, 87(2005), P.511-519
13. Z.G. Wu, C.X. Zhou, R.R. Qi and H.B. Zhang, *J Appl Polym Sci* **83** (2002), p. 2403. |
14. H.L. Tyan, Y.C. Liu and K.H. Wei, *Polymer* **40** (1999) (17), p. 4877.
15. T. Lan, P.D. Kaviratna and T.J. Pinnavaia, *J Phys Chem Solids* **57** (1996), p. 6.
16. J. Ma, S. Zhang and Z.N. Qi, *J Appl Polym Sci* **2** (2001) (6), p. 1444.
17. Y.C. Ke, C.F. Long and Z.N. Qi, *J Appl Polym Sci* **71** (1999), p. 1139.
18. J. B. Donnet, Composites Science and Technology, **63,** (2003) pp1085-1088.